JACS
JOURNAL OF THE AMERICAN CHEMICAL SOCIETY

Communication

pubs.acs.org/JACS

Superatom Electron Configuration Predicts Thermal Stability of $Au_{25}(SR)_{18}$ Nanoclusters

Marcus A. Tofanelli and Christopher J. Ackerson*

Department of Chemistry, Colorado State University, Fort Collins, Colorado 80523, United States

Supporting Information

ABSTRACT: The exceptional stability of ligand-stabilized gold nanoclusters such as $Au_{25}(SC_6H_{13})_{18}^-$, $Au_{39}(PR_3)_{14}X_6^-$, and $Au_{102}(SR)_{44}$ arises from the total filling of superatomic electron shells, resulting in a "noble-gas superatom" electron configuration. Electrochemical manipulation of the oxidation state can add or remove electrons from superatom orbitals, creating species electronically analogous to atomic radicals. Herein we show that oxidizing the $Au_{25}(SR)_{18}^-$ superatom from the noble-gas-like $1S^21P^6$ electron configuration to the open-shell radical $1S^21P^5$ and diradical $1S^21P^4$ configurations results in decreased thermal stability of the compound, as measured by differential scanning calorimetry. Similar experiments probing five oxidation states of the putatively geometrically stabilized $Au_{144}(SR)_{60}$ cluster suggest a more complex relationship between oxidation state and thermal stability for this compound.

The electron configurations of elements predict a remarkable set of properties, including ionization energy, electronegativity, and bonding valency. The superatomic electron configurations of metal clusters predict stable molecular formulas, which are associated with noble-gas-like superatomic electron configurations.[1,2] Geometric shell closing can also stabilize metal nanoclusters, making electronic and geometric shell closures competing modes of nanoparticle stabilization. Smaller nanoparticles tend toward stabilization by superatomic shell closing, while larger nanoparticles tend toward stabilization by geometric shell closing.[3] The theory of metal clusters as electronic superatoms has been most widely deployed for gas-phase clusters.[4]

The extension of superatom theory from gas-phase clusters to soluble, stable, ligated clusters is recent[1] and has been best developed for ligated gold nanoclusters,[5,6] although it is being increasingly applied to ligated clusters of other transition metals.[7] Structural and theoretical data for gold−thiolate nanocluster compounds suggest that geometric shell closures dominate the stability of $Au_{144}(SR)_{60}$ and larger,[8−11] while electronic shell filling stabilizes $Au_{102}(SR)_{44}$ and smaller.[12,13]

The solution of the Schrodinger equation for a spherically symmetric square-well potential defines the superatomic orbitals for approximately spherical particles.[2] The spherical superatom orbitals are 1S, 1P, 1D, 2S 1F, 2P 1G, 2D 1H 3S, ... Thus, the electron counts that achieve a particularly stable (noble-gas-like) configuration are 2, 8, 18, 34, 58, 92, ... For a metal cluster formulated as $(L_s{\cdot}A_NX_M)^z$, where A and X represent metal atoms and electron-withdrawing ligands with N and M being their respective numbers, L represents dative ligands, s the number of dative ligands, and z represents the overall charge on the compound, the number of superatomic electrons is

$$n^* = NV_A - M - z \quad (1)$$

where V is the valence of the metal atom ($V = 1$ for Au, which donates its 6s electron). When n^* is equivalent to the number of electrons required to close a superatomic shell (i.e., a magic number), special stability is observed, analogous to the special stability of noble gases.

Implicit in the superatom description of nanoclusters is that filled electronic shells produce highly inert, noble-gas-like compounds, while open-shell compounds may be more reactive. Castleman and Khanna extended the superatom theory to show that ion pairs[14] and extended solid-state networks[15,16] can be formed from open-shell Al and As clusters that are soft-landed from the gas phase.

Compared with the work on soft-landed gas-phase clusters, the application of superatom theory to ligated clusters is more limited and to date has been used in two notable ways. First, superatom theory has been used to explain the special stability of compounds such as $Au_{25}(SR)_{18}^-$, $Au_{39}(PPh_3)_{14}Cl_6^-$, $Au_{68}(SR)_{34}$, and $Au_{102}(SR)_{44}$ as resulting from total fillings of the 2P, 1F, 1F, and 1G shells (i.e., n = 8, 34, 34, and 58), respectively.[1,13,17−21] Second, the observed paramagnetism of the $Au_{25}(SR)_{18}^0$ species has been explained in terms of an unpaired superatomic electron arising in a $1S^2\ 1P^5$ superatomic electron configuration.[6,17]

Here we performed a direct experimental test of the superatom theory as applied to ligated metal clusters and established that superatomic electron configurations of $Au_{25}(SC_6H_{13})_{18}$ are predictive of the thermal decomposition temperature of this compound. For comparison, we also established the thermal stability of charge states of the putatively geometrically stabilized[8,22] compound $Au_{144}(SC_6H_{13})_{60}$.

$Au_{25}(SC_6H_{13})_{18}$ and $Au_{144}(SC_6H_{13})_{60}$ were prepared by the methods of Murray[23] and Jin,[24] respectively, with minor modifications, as detailed in the Supporting Information (SI). Differential pulse voltammetry (DPV) was done on a Bioanalytical Systems BAS 100B potentiostat using 100 mmol of tetrabutylammonium hexafluorophosphate ($TBAPF_6$) or ca. 50 mmol of tetraethylammonium tetrafluoroborate ($TEABF_4$)

Received: July 24, 2012
Published: September 26, 2012

dx.doi.org/10.1021/ja3072644 | J. Am. Chem. Soc. 2012, 134, 16937−16940

as the electrolyte in dichloromethane (DCM) solvent, similar to the previous work of Murray.[25−29] Bulk electrolysis was performed under air in a two-frit, three-chamber electrochemical cell and controlled by the same potentiostat used for the DPV experiments. Differential scanning calorimetry (DSC) was accomplished using a TA Intruments 2920 modulated differential scanning calorimeter. All products were redissolved in a minimal amount of DCM and then deposited into an aluminum hermetic DSC pan and allowed to air-dry in order to achieve uniform coverage of the pan. Vacuum was applied for 10 min to ensure complete removal of DCM. Additional experimental details may be found in the SI.

We prepared $Au_{25}(SC_6H_{13})_{18}$ in the −1, 0, and 1 charge states and $Au_{144}(SC_6H_{13})_{60}$ in the −1, 0, 1, 2, and 3 charge states. The preparation of each formal charge state proceeded by initial collection of a differential pulse voltammogram and verification that the as-prepared clusters showed the expected electrochemical response (Figure 1). Following the DPV measurement, analytical amounts (1−3 mg) of each cluster in each targeted formal charge state were prepared by bulk electrolysis. To isolate the stability effect of the cluster core charge from the effect of counterions, we executed bulk electrolysis with two different electrolytes, $TBAPF_6$ and $TEABF_4$. Success of the bulk electrolysis preparation was verified by resting potential measurements. The integrity of the electrolyzed cluster preparations was also confirmed by postelectrolysis DPV measurements, and in the case of $Au_{25}(SC_6H_{13})_{18}$, additional confirmation was provided by the fact that the spectra we observed for various charge states reproduced the spectra measured in other laboratories (Figure 1 inset).[30,31] Analyses of $Au_{25}(SC_6H_{13})_{18}$ in the +2 or −2 charge state were not attempted because of the apparent instability of the cluster in these charge states; In fact, even the +1 charge state required careful handling (Figure S3 in the SI). More negative formal charges for Au_{144} were difficult to prepare stably because of our inability to exclude oxygen from the calorimeter completely, while more positive charge states of Au_{144} appeared to revert spontaneously to lower formal charge states during the course of the experiment as judged by resting potential measurements.

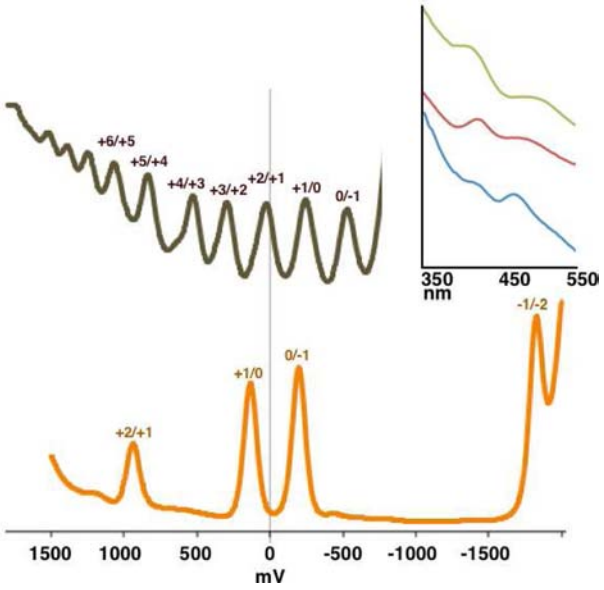

Figure 1. DPV data for the as-prepared $Au_{25}(SR)_{18}$ (orange) and $Au_{144}(SR)_{60}$ (brown). Potentials are relative to the standard calomel electrode. The inset shows the relative UV/vis absorbance spectra of bulk electrolysis preparations of $Au_{25}(SR)_{18}$ in the −1, 0, and +1 charge states (blue, red, and green, respectively).

$Au_{25}(SC_6H_{13})_{18}$ should be most stable in the $1S^21P^6$ configuration, corresponding to the molecular anion. Thus, the superatomic electron configurations of the three $Au_{25}(SC_6H_{13})_{18}$ species that we prepared are $1S^21P^6$, $1S^21P^5$, and $1S^21P^4$. The thermal characteristics, including the thermal stability, of $Au_{25}(SC_6H_{13})_{18}$ in each of these electron configurations were measured in DSC experiments. For every compound tested there was a major thermal event, corresponding to what we believe to be the desorption of the ligand shell and subsequent decomposition of the cluster. We interpret the temperature at which this major thermal event occurs as an indicator of the thermal stability of the cluster; clusters that decompose at higher termperatures are thus more thermally stable. By this metric of stability, $Au_{25}(SC_6H_{13})_{18}^-$ (with the noble-gas-like superatomic electron configuration) is more stable than the $Au_{25}(SC_6H_{13})_{18}^0$ radical, which in turn is more stable than the $Au_{25}(SC_6H_{13})_{18}^+$ superatomic diradical (Figure 2), with each additional electron removal causing ca. 10 °C of destabilization. At least three measurements were made for each preparation.

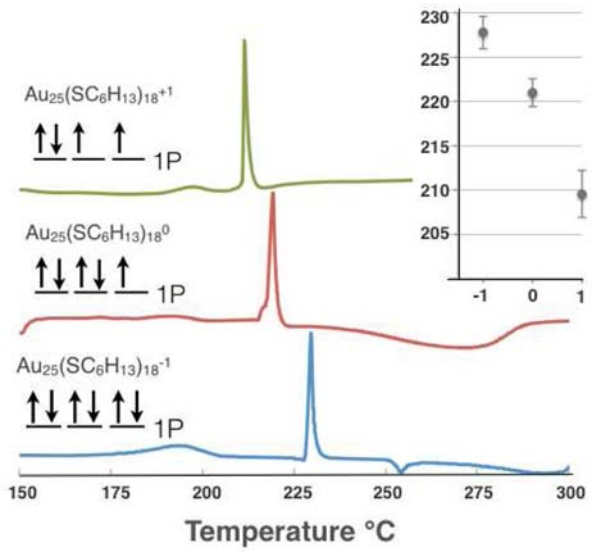

Figure 2. DSC curves for the −1, 0, and +1 charge states of $Au_{25}(SC_6H_{13})_{18}$ (blue, red, and green, respectively). The temperatures of the corresponding thermal decomposition events for the three charge states (227.5, 221, and 209 °C) are plotted in the inset.

For the $Au_{25}(SC_6H_{13})_{18}^0$ and $Au_{25}(SC_6H_{13})_{18}^+$ charge states, different electrolytes gave indistinguishable stability measurements when the standard error was taken into account. The $Au_{25}(SC_6H_{13})_{18}^-$ charge state appeared to be slightly stabilized by the tetrabutylammonium counterion relative to the tetramethylammonium or tetraethylammonium counterion, although the effect of the electrolyte was small in comparison with the effect of the charge state. The Figure 2 inset reports the results of the DSC runs for all of the electrolytes with standard error. Figure S2 shows the separate effects of the electrolyte and charge on the thermal stability.

dx.doi.org/10.1021/ja3072644 | J. Am. Chem. Soc. 2012, 134, 16937−16940

We also measured the charge-state-dependent thermal stability of $Au_{144}(SC_6H_{13})_{60}$ for the five prepared charge states of this compound. The charge state and thermal stability do not appear to be closely linked for this compound (Figure 3)

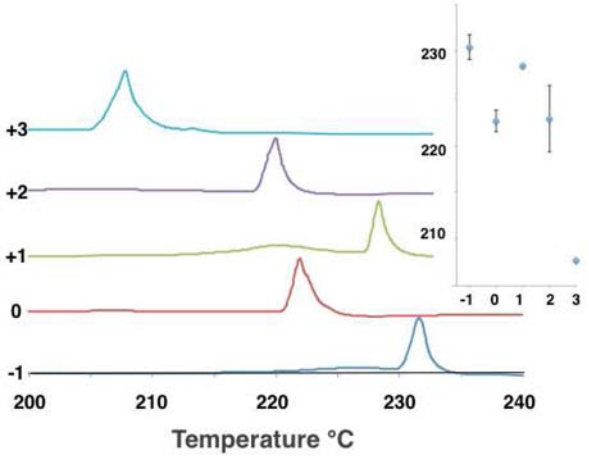

Figure 3. DSC curves for representative samples of $Au_{144}(SC_6H_{13})_{60}$ in the +3, +2, +1, 0, and −1 oxidation states. The inset shows the mean decomposition temperature for multiple measurements at each oxidation state, with error bars representing the standard deviation for the set of measurements. Only one measurement was made for the +3 oxidation state.

Moreover, the counterion retained by the $Au_{144}(SC_6H_{13})_{60}$ nanocluster after bulk electrolysis could in many cases exert a dramatic effect on the nanocluster thermal stability (data not shown), consistent in part with the description of this compound as stabilized in part by an electrical double layer.[32] While superatomic orbital effects are presently not considered to be as important as the filling of geometric closed shells for conferring stability to $Au_{144}(SC_6H_{13})_{60}$, we suggest below how superatomic electron effects may account in an unpredictable manner for the absence of a trend in the thermal stability as a function of oxidation state for $Au_{144}(SC_6H_{13})_{60}$.

Geometric stabilization of $Au_{144}(SC_6H_{13})_{60}$ is suggested by a widely cited density functional theory (DFT) model of $Au_{144}(SC_6H_{13})_{60}$,[8] by the inexplicability of the cluster's formula and electronic structure in terms of superatom theory,[1] and by the observation of a single symmetry environment by NMR spectroscopy, which is consistent with the DFT model.[10,28] In contrast, superatomic-stabilized clusters show multiple symmetry environments as judged by NMR spectroscopy.[10] The ligand symmetry environment of $Au_{144}(SC_6H_{13})_{60}$ appears to change reversibly upon oxidation and reduction of the $Au_{144}(SC_6H_{13})_{60}$ cluster.[28] Taken together, the unpredictable counterion- and charge-dependent thermal stability and the apparent breakdown of symmetry in some oxidation states leads us to speculate that residual superatom electronic effects may provoke Jahn−Teller-type distortion of these structurally obscure clusters. This means that competing superatomic effects may alter the structure and electronic and thermal stability of these clusters in unpredictable ways that depend on the interplay of geometric, ligand-steric, and electronic effects.

In contrast to $Au_{144}(SC_6H_{13})_{60}$, the outer coordination shell [SR−Au(I)−SR−Au(I)−SR units] of $Au_{25}(SC_6H_{13})_{18}$ may act in concert with the organic ligands of this cluster to constrain the geometry even when the superatomic electron configuration favors Jahn−Teller-type distortion. Thus, there are no significant distortions between $Au_{25}(SC_6H_{13})_{18}^{-}$ and $Au_{25}(SC_6H_{13})_{18}^{0}$ in single-crystal X-ray structures,[13,18,33] while we observe stability trends predicted by the superatomic electron configuration. While the low rates of electron transfer for $Au_{25}(SR)_{18}^{0/-1}$ noted by Murray and Maran[30] suggest a charge-state-dependent distortion, the totality of current evidence suggests that this distortion is small.

In conclusion, we have shown that the superatom electron configuration predicts a thermal stability trend for noble-gas, radical, and diradical superatom electron configurations of $Au_{25}(SR)_{18}$. Clear trends were not observed for $Au_{144}(SR)_{60}$, leading us to speculate that a complex interplay of electronic and geometric effects may be of importance. The extension of superatom theory to predict other properties of ligated clusters, such as superatomic valency and catalytic reactivity, remain largely open questions.

■ ASSOCIATED CONTENT

Supporting Information

Full DSC curves, additional data on the effect of the counterion on thermal stability, data on $Au_{25}(SR)_{18}^{+}$ instability, and expanded experimental details. This material is available free of charge via the Internet at http://pubs.acs.org.

■ AUTHOR INFORMATION

Corresponding Author

ackerson@colostate.edu

Notes

The authors declare no competing financial interest.

■ ACKNOWLEDGMENTS

The authors thank Colorado State University for funding this work. This work was accomplished while C.J.A. was an American Federation for Aging Research New Investigator. The authors thank Hannu Häkkinen for useful conversations on superatom theory and C. Michael Elliott for use of electrochemistry equipment and generous advice.

■ REFERENCES

(1) Walter, M.; Akola, J.; Lopez-Acevedo, O.; Jadzinsky, P. D.; Calero, G.; Ackerson, C. J.; Whetten, R. L.; Grönbeck, H.; Häkkinen, H. *Proc. Natl. Acad. Sci. U.S.A.* **2008**, *105*, 9157−9162.
(2) de Heer, W. A. *Rev. Mod. Phys.* **1993**, *65*, 611−676.
(3) Martin, T. P.; Bergmann, T.; Göhlich, H.; Lange, T. *J. Phys. Chem.* **1991**, *95*, 6421−6429.
(4) Castleman, A. W., Jr. *J. Phys. Chem. Lett.* **2011**, *2*, 1062−1069.
(5) Häkkinen, H. *Chem. Soc. Rev.* **2008**, *37*, 1847−1859.
(6) Zhu, M.; Aikens, C. M.; Hendrich, M. P.; Gupta, R.; Qian, H.; Schatz, G. C.; Jin, R. *J. Am. Chem. Soc.* **2009**, *131*, 2490−2492.
(7) Clayborne, P. A.; Lopez-Acevedo, O.; Whetten, R. L.; Grönbeck, H.; Häkkinen, H. *Eur. J. Inorg. Chem.* **2011**, 2649−2652.
(8) Lopez-Acevedo, O.; Akola, J.; Whetten, R. L.; Grönbeck, H.; Hakkinen, H. *J. Phys. Chem. C* **2009**, *113*, 5035−5038.
(9) Dass, A. *J. Am. Chem. Soc.* **2011**, *133*, 19259−19261.
(10) Wong, O. A.; Heinecke, C. L.; Simone, A. R.; Whetten, R. L.; Ackerson, C. J. *Nanoscale* **2012**, *4*, 4099−4102.
(11) Qian, H.; Zhu, Y.; Jin, R. *Proc. Natl. Acad. Sci. U.S.A.* **2012**, *109*, 696−700.
(12) Lopez-Acevedo, O.; Tsunoyama, H.; Tsukuda, T.; Häkkinen, H.; Aikens, C. M. *J. Am. Chem. Soc.* **2010**, *132*, 8210−8218.
(13) Zhu, M.; Aikens, C. M.; Hollander, F. J.; Schatz, G. C.; Jin, R. *J. Am. Chem. Soc.* **2008**, *130*, 5883−5885.
(14) Bergeron, D. E.; Castleman, A. W., Jr.; Morisato, T.; Khanna, S. N. *Science* **2004**, *304*, 84−87.

(15) Castleman, A. W., Jr.; Khanna, S. N. *J. Phys. Chem. C* **2009**, *113*, 2664−2675.
(16) Claridge, S. A.; Castleman, A. W., Jr.; Khanna, S. N.; Murray, C. B.; Sen, A.; Weiss, P. S. *ACS Nano* **2009**, *3*, 244−255.
(17) Nealon, G. L.; Bertrand Donnio, B.; Greget, R.; Kappler, J.; Terazzi, E.; Gallani, J. *Nanoscale* **2012**, *4*, 5244−5258.
(18) Heaven, M. W.; Dass, A.; White, P. S.; Holt, K. M.; Murray, R. W. *J. Am. Chem. Soc.* **2008**, *130*, 3754−3755.
(19) Teo, B.; Shi, X.; Zhang, H. *J. Am. Chem. Soc.* **1992**, *114*, 2743−2745.
(20) Dass, A. *J. Am. Chem. Soc.* **2009**, *131*, 11666−11667.
(21) Jadzinsky, P. D.; Calero, G.; Ackerson, C. J.; Bushnell, D. A.; Kornberg, R. D. *Science* **2007**, *318*, 430−433.
(22) Kumara, C.; Dass, A. *Nanoscale* **2011**, *3*, 3064−3067.
(23) Parker, J. F.; Weaver, J. E. F.; McCallum, F.; Fields-Zinna, C. A.; Murray, R. W. *Langmuir* **2010**, *26*, 13650−13654.
(24) Qian, H.; Jin, R. *Chem. Mater.* **2011**, *23*, 2209−2217.
(25) Chen, S.; Ingram, R. S.; Hostetler, M. J.; Pietron, J. J.; Murray, R. W.; Schaaff, T. G.; Khoury, J. T.; Alvarez, M. M.; Whetten, R. L. *Science* **1998**, *280*, 2098−2101.
(26) Ingram, R. S.; Hostetler, M. J.; Murray, R. W.; Schaaff, T. G.; Khoury, J. T.; Whetten, R. L.; Bigioni, T. P.; Guthrie, D. K.; First, P. N. *J. Am. Chem. Soc.* **1997**, *119*, 9279−9280.
(27) Garcia-Raya, D.; Madueno, R.; Blazquez, M.; Pineda, T. *J. Phys. Chem. C* **2009**, *113*, 8756−8761.
(28) Song, Y.; Harper, A. S.; Murray, R. W. *Langmuir* **2005**, *21*, 5492−5500.
(29) Quinn, B. M.; Liljeroth, P.; Ruiz, V.; Laaksonen, T.; Kontturi, K. *J. Am. Chem. Soc.* **2003**, *125*, 6644−6645.
(30) Parker, J. F.; Fields-Zinna, C. A.; Murray, R. W. *Acc. Chem. Res.* **2010**, *43*, 1289−1296.
(31) Venzo, A.; Antonello, S.; Gascón, J. A.; Guryanov, I.; Leapman, R. D.; Perera, N. V.; Sousa, A.; Zamuner, M.; Zanella, A.; Maran, F. *Anal. Chem.* **2011**, *83*, 6355−6362.
(32) Murray, R. W. *Chem. Rev.* **2008**, *108*, 2688−2720.
(33) Zhu, M.; Eckenhoff, W. T.; Pintauer, T.; Jin, R. *J. Phys. Chem. C* **2008**, *112*, 14221−14224.